New generation of PVD coated rings for high performance flex fuel engines

Felipe Mazuco*
Luiz Felipe Rezende
Rafael Bruno
MAHLE, Rodovia Anhanguera, km 49,7, 13.210-877 Jundiaí, SP, Brazil

Dr. Juliano Araujo
MAHLE Componentes de Motores SA, Núcleo Industrial de Murtede, 3060-372 Murtede, Portugal

RESUMO

Um problema já conhecido para revestimentos de anel de pistão em combinação com o uso de etanol são as micro trincas e destacamentos localizados. Melhorias nos revestimentos de CrN foram feitas junto com o desenvolvimento dos motores flex. No entanto, com a introdução de novas legislações no Brasil para aumentar a eficiência dos motores e reduzir as emissões, as montadoras foram levadas a atualizarem seus motores em termos de hardware e calibração levando a maiores cargas termomecânicas. Os revestimentos de CrN otimizados foram impactados diretamente pelo ambiente tribológico severo e retornaram a sofrer ocorrências de micro trincas e de destacamentos localizados.

Este trabalho aborda a última geração de revestimentos de PVD, dopando o CrN com Alumínio e adotando uma estrutura em nanocamadas. O Nitreto de Cromo Alumínio (CrAlN) oferece dureza superior, estabilidade térmica e química aumentadas e a coesão melhorada do revestimento. A arquitetura em nanocamadas, conseguida através da modulação do teor de alumínio, atua como uma barreira para a propagação de trincas. Testes de motor confirmaram que o novo revestimento permanece livre de micro trincas e destacamentos, mesmo sob condições motores flex-fuel altamente carregados.

ABSTRACT

A well-known issue with piston ring coatings in combination with ethanol use is the occurrence of microcracks and spalling. Specific improvements in the CrN coatings were made along with the flex fuel engines development. However, the introduction of new legislations in Brazil to increase engine efficiency and lower emissions led the automakers to upgrade their engines in terms of hardware and calibration with the consequence of increased thermomechanical loads. The improved CrN coatings were directly impacted by such harsher tribological environment returning to suffer from microcracks and spalling occurrences.

The latest generation of PVD coatings addresses these challenges by incorporating aluminum into CrN and adopting a nanolayered structure. Chromium Aluminum Nitride (CrAlN) offers superior hardness, enhanced thermal and chemical stability, and improved coating toughness. The nanolayered architecture, achieved through modulation of the aluminum content, acts as a barrier for crack propagation. Engine tests have confirmed that the new coating remains free from microcracks and spalling, even under high-load conditions in flex-fuel engines.

INTRODUCTION

Since the development of the first flex fuel engine generation, a lot of improvements have been made to the engine components and the associated sub-systems. These product adaptations might be necessary from either design and/or materials aspects. Some of these changes were somehow predictable, whereas some others were only realized during the development or after the implementation of the Flex Fuel Engines to the market.

For piston rings, one of the most important product adaptations necessary to adequate to the flex fuel environment was related to the top ring running face coating. The new boundary technical conditions – which will be better explained and explored in this article – led the rings to a tribological condition not existing so far [1].

The scope of this article approaches specifically the CrN coating deposited by PVD, largely applied to light vehicle engines worldwide. Since the first generation of flex fuel engines, the need of improvement of the original CrN coating has been noticed. An improved CrN coating was developed and has been successfully applied since then [1].

Now, to cope with the new emission / fuel efficiency regulations, OEMs had to adjust their engine calibrations, promoting again a harsher tribological environment to piston rings and then demanding a new upgrade on top ring coatings. The work aims to describe the development of the CrAlN multilayer coating and show its results regarding hardness, wear, microstructure and microcracks resistance.

MOTIVATION – COATING FAILURES

Several technical aspects bring further tribological challenges for piston rings when working in an ethanol fueled engine. First of them is the higher fuel amount injected in the cylinder, which leads to increased fuel dilution into lube oil, so that degrading the lube oil lubricity and viscosity. Not talking about the potential chemical attack effects, which may attack some engine component materials, the rheology of the lubricant itself gets worsened due to this increased fuel dilution [2].

In addition to this effect, another challenge brought by the use of ethanol fuel (E100) is the increment of the Peak Cylinder Pressure (PCP) as compared E22, as indicated by Figure 1. It is noticeable that the peak pressure happens closer to the piston top dead center, so that in a position where the piston presents lower sliding velocity, consequently less hydrodynamic support, which means more intensive contact of surface asperities (ring / liner). The curves presented Figure 1 represent a natural aspirated, PFI engine. Modern flex fuel engines are usually turbo charged and most of them already applying Direct Inject (DI) system, which makes the tribological environment even harsher.

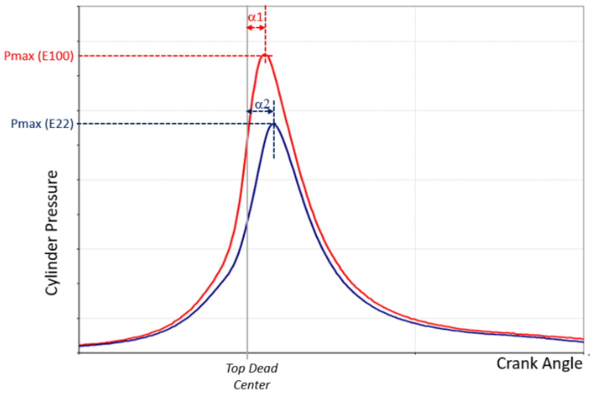

Figure 1 - Cylinder pressure curves (adapted from [1])

As consequence of such an aggressive tribological system, top ring coatings are exposed to thermomechanical fatigue, especially at the ring's contact surfaces, and propagate under cyclic loads which may lead to surface microcracks network or, on more severe cases, spalling occurrence. Spalling is a partial detachment of the coating layer, as consequence of a cohesive failure caused by the micro-fatigue action. Both microcracks and spalling occurrences are illustrated on Figure 2. The microcracks occurrences were seen in multiple engines (PFI and DI) after 100h to 500h tests at dynamometer and after vehicle testing. In all cases the fuel used was ethanol (E100). No occurrences were reported when gasoline (E22/E27) was used.

It is important to make clear that so far, no engine functional failure or performance jeopardy has been associated or caused by any of these occurrences (micro-cracks nor spalling). However, the surface deterioration is an indication that the coating is reaching its technical application limit, so that an improvement must be made on the coating in order to allow the component to be prepared and withstand further technical demands expected for the next engine generations.

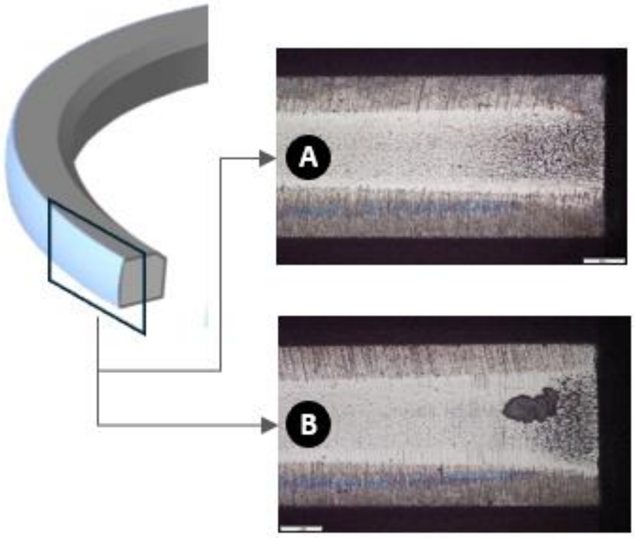

Figure 2 - Representative pictures of (A) microcrack network and (B) spalling occurrence on top ring running face.

NANOSTRUCTURED MULTILAYER COATINGS

In recent years, coatings based on transition metal compounds (metal nitrides) such as Chromium Nitride [3] and Titanium Aluminum Nitride [4] have attracted considerable attention due to their corrosion resistance. Additionally, different ceramic/ceramic nanostructured multilayer systems have been explored by industrial communities due to their enhanced properties compared to those usually found in the corresponding individual monolayer nitride coatings, resulting in mechanical and tribological improvements. For example, CrN/NbN [5] and TiN/NbN [6-8] have been employed as protective coatings on tools and other mechanical parts used in tribological applications.

In this context, the approach of combining nanostructured multilayer coatings with metals has been extended to CrN/CrAlN, aiming to combine the wear resistance of CrN with the appropriate selection of Al as a partner material, as shown by Mani et al. where CrAlN mainly crystallizes in a CrN face-centered cubic lattice structure, but with a decreased lattice parameter compared to CrN [9]. This can introduce a suitable strain and maintain a coherent interface between the layers [10–12].

A higher number of interfaces (lower periodicity) and sharp boundaries between the CrN and CrAlN sub-layers can serve as a useful microstructural marker, helping to delay cohesive delamination [3]. This benefit has previously been qualitatively correlated with a reduction in the wear rate of the coating [13,14].

In monolayer coatings, a defective interfacial region weakens the load-bearing capacity, leading to the easy development of tensile cracks and premature delamination, which harms the coating's performance. Therefore, one possible reason for the increased resistance to failure at low periodicity (a few nanometers) could be the strong crystallographic texture of the coatings, combined with well-defined interfaces between the individual components. The larger number of interfaces and sharp edges between the CrN and CrAlN layers contribute to material removal within the nanoscale layers [15,16], leading to reduced wear rate and increased cohesive integrity.

It is important to note that most of the available literature focuses on coatings with a thickness of less than 6 µm, typically deposited by sputtering. In contrast, the coating in this work has a thickness greater than 25 µm. Regarding deposition processes, cathodic arc deposition has industrial relevance due to its higher deposition rate compared to sputtering. Sputtering can be economically restrictive when comparing deposition rates (Sputtering/HIPIMS: ~1.2 µm/hr) [17,18] to the ARC process (~3.0 µm/hr) [19].

PROCESS DEPOSITION - CrAlN Multilayer

Deposition was conducted in an industrial cathodic arc physical vapor deposition equipment where 4 metallic targets made of Chromium and Aluminum (Low Aluminum < 10 %at.) are assembled in one side and 4 other metallic targets also made of Chromium and Aluminum (High Aluminum > 30% at.) are assembled in the other side as per Figure 3. The metallic targets are disks of 150 mm diameter and 30mm thickness with high purity (>99.7%) and are each assembled in its cathode position, powered individually by a DC power supply.

Piston rings are assembled in the planetary substrate table stacked in axial direction forming the ring arbor. The arbors are subject to 2-fold movement (rotation on table and arbor axis) to ensure optimal thickness distribution and to achieve desired periodicity of the nanostructured coating.

The deposition is structured as it follows:

1. Pumping and heating.
2. Ion etching process for removal of impurities [20].
3. Bond layer coating to provide a transition of mechanical properties [21].
4. Functional coating – CrAlN Multilayer.

Process atmosphere alternates between Argon (non-reactive) and Nitrogen (reactive) throughout the process.

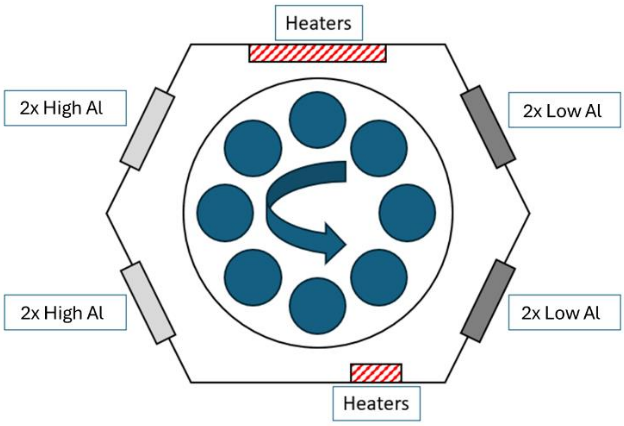

Figure 3 – General disposition of PVD equipment

COATING DETAILS – CrAlN Multilayer

THICKNESS AND MORPHOLOGY – A piston ring cross section micrography was taken by Scanning Electron Microcopy (SEM) to evaluate the thickness and morphology as shown in the Figure 4. The coating is formed of a 0,5 µm chromium adhesion layer and 15 µm of CrAlN multilayer coating. Both layers were deposited onto a gas nitrided steel (GNS) widely used for piston rings [1]. The total thickness of the coating can be adjusted using the deposition time and the current setup can reach up to 45 µm thickness. The CrAlN coating morphology is dense with low porosity level and few droplets. Droplets are formed as a result of ejection of liquid metal particles from the target material, compatible with the cathodic arc deposition [22].

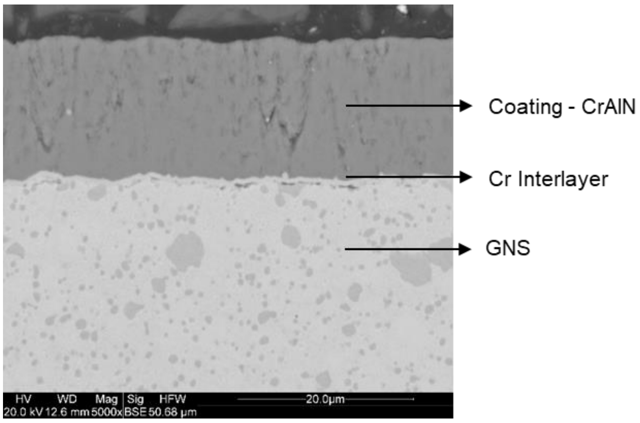

Figure 4 - Cross section of CrAlN coating by SEM.

NANOSTRUCTURE – The nanostructure of the coating was analyzed by Transmission Electron Microscopy (TEM), using a Titan Cubed Themis microscope operating at an accelerating voltage of 300 kV. The microscope was operated in Scanning Transmission Electron Microscopy (STEM) mode with a 115 mm long camera. The STEM was adopted for image acquisitions using the High-Angle Annular Dark-Field (HAADF) to enable that the images have an enhanced mass-thickness contrast, which means that the heavier elements appear brighter. TEM specimens were prepared using a Focused Ion Beam (FIB) lift-out method in FEI Helios Nano lab 660 (Dual Beam) equipment. A procedure similar to that reported in Meng-Burany et al. [23] was conducted. The region used for the nanolayers measurement was about 5 µm below the surface as shown in the Figure 5.

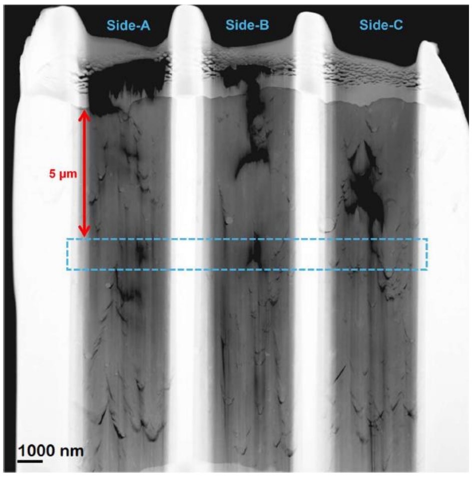

Figure 5 - Image of the specimen by STEM-HAADF with low amplification.

The Figure 6 shows a representative image of the nanolayers of the CrAlN coating. The nanolayer structure is a direct result of the two-fold rotation used in the substrate holder in the PVD machine and the use of two different target materials with different Al content. The brighter layer is a CrAlN with lower Al content while the darker layer is a CrAlN with higher Al content. It also can be highlighted that the darker layer is slightly thicker than the brighter layer. For the measurement of the periodicity (sum of both sub-layers), a profile based on the brightness was generated as shown in Figure *7*. The periodicity ranged from 3 to 30 nm, depending on the table rotation.

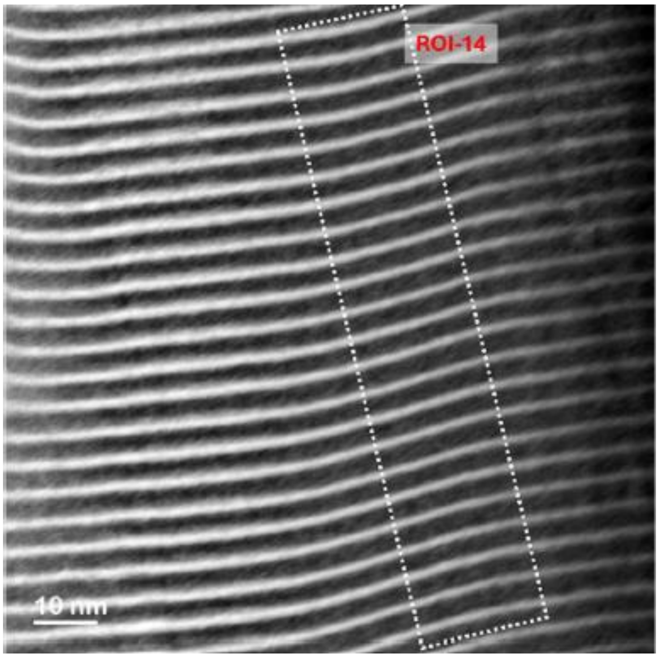

Figure 6 - Nanolayers image obtained by STEM-HAADF.

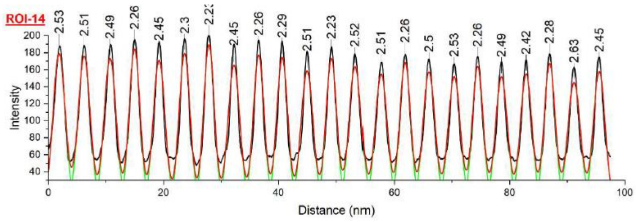

Figure 7 - Profile of the nanolayers based on the brightness

HARDNESS – The hardness of the coating was measured on the cross section of the five samples with two different techniques: conventional Vickers microhardness and instrumented indentation using a commercial nano-indenter, Anton Paar NHT3®. For the instrumented indentation the measurements were conducted with a Berkovich type indenter and properties were calculated using the Oliver & Pharr method [24]. The average of 10 valid measurements was taken.

Table 1 presents the hardness results. The hardness obtained ranged from 1974 HV to 2114 HV by microhardness. The values obtained are higher than the hardness observed for CrN coatings used for piston rings, which range from 1000 to 1400 HV [25]. The increase in hardness compared with pure CrN can be explained by the solid solution of aluminum in the CrN structure that deforms the lattice [26] and by the nanolayers effect that difficult the dislocations movement [27]. Although the values are lower than that reported by Araujo et al. [28] of 3200 HV for NbN/CrN coatings with similar periodicity of 4 nm. The main reason for such difference is the proximity of the lattice parameters of the sub-layers formed [29].

The hardness obtained by instrumented indentation ranged from 22,3 up to 24,0 GPa. The values are similar to those reported for CrN/CrAlN multilayer coatings produced by magnetron sputtering [30] but lower than the DLC coatings also used for piston rings, which are around 32 GPa [31].

Table 1 - Hardness measurements.

Technique	**Microhardness**	**Instrumented Indentation**
Load details	*25 g*	*HIT 0.002/30/0/30*
Hardness Unit	*HV*	*GPa*
Sample 1	2050	24,0
Sample 2	2023	22,9
Sample 3	2114	23,3
Sample 4	1974	22,4
Sample 5	2005	22,3

BENCH TESTING

WEAR – The wear evaluation was performed at Bruker's Universal Mechanical Tester (UMT). The test consists of a 360N normal load applied for 4 hours on the ring running against a liner coupon flooded in oil (SAE 0W20). The ring sample reciprocates over the liner surface with a stroke of 10 mm at 15 Hz frequency. To accelerate ring wear, the oil is doped with hard alumina particles. Ring and liner wear are measured by comparing the respective profile, before and after test.

The wear performance of CrAlN multilayer was compared with CrN and DLC coatings that are competing solutions for piston rings. The results are shown in the Figure 8. The CrAlN multilayer coating have achieved a 50% ring wear reduction over the CrN, from 6 to 3 µm, maintaining the same liner wear of 1,5 µm. The reduction in wear can be accounted for the increase in hardness and to the existence of a larger number of interfaces between CrAlN layers [15,16]. The DLC presented a wear reduction of 75% over the CrN but with an increase in the liner wear from 1,5 to 2,5 µm.

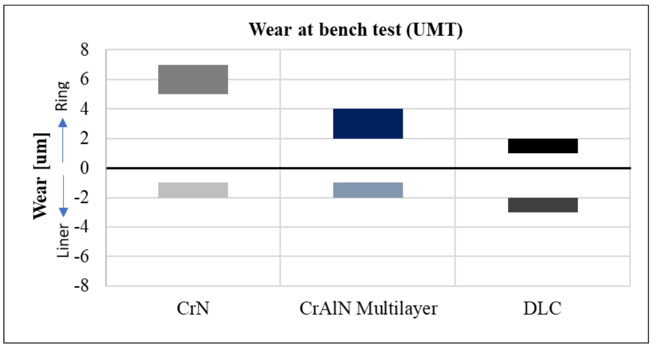

Figure 8 - Wear at bench test (UMT)

SCUFFING – The scuffing test was performed in the Optimal Instruments SRV tribometer (in german, "Schwing Reib Verschleiss", that means oscillation, friction, wear). The procedure consists of a reciprocating rig test with load, frequency, angle and temperature control, as well as friction coefficient measurements through a pair of load cells. Oil injection is controlled with a high precision pump. The equipment and sketch are shown in Figure 9.

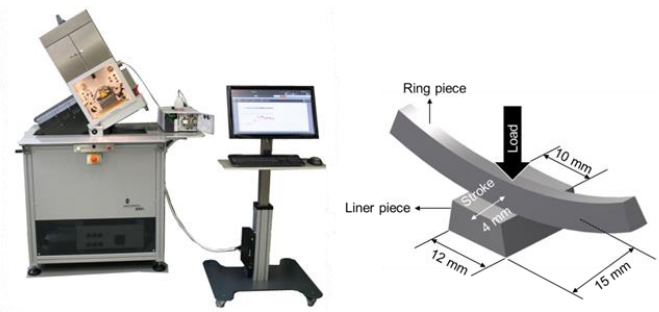

Figure 9 - Scuffing test equipment and sketch of the test

The procedure used is based in the work from Obert et al. [32] and detailed in the Table 2. The test has the duration of 6 hours in each load. The failure criterion is the friction coefficient above 0.3 over than 30 seconds. If the test passed after the 6h, a new test is performed with a load increase of 25N. The scuffing limit is expressed as the Load Carrying Capacity (LCC) that is calculated based in the maximum load that the coating withstood without failure.

Table 2 - Scuffing test procedure at SRV.

Temperature	210°C
Oil flow	0.1 µL/min
Oil	SAE 0W-20
Stroke	4 mm
Frequency	20 Hz
Angle	45°
Load step	25N

The scuffing resistance results for the CrN, CrAlN multilayer and DLC are presented in Figure 10. The CrN coating exhibited the lowest performance, with a LCC of 200 N. The CrAlN multilayer demonstrated a moderate improvement, with a LCC of 275 N. In contrast, the DLC coating showed the highest resistance to scuffing, achieving a LCC of 600 N. These results indicates that the DLC coating offers superior protection against scuffing which enables the use of low viscosity oils. The CrAlN multilayer did not bring any demerit against scuffing when compared with the CrN coating.

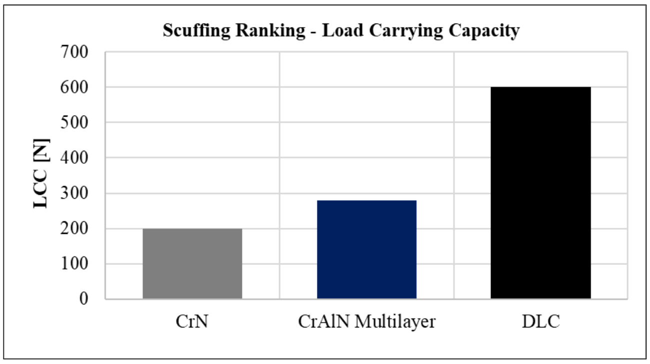

Figure 10 - Scuffing resistance results

ENGINE TEST

To evaluate the microcracks and spalling occurrences an engine test in a high-loaded flex engine was performed.

ENGINE AND TEST DETAILS – The engine was chosen based on the high level of microcracks that were observed for the current coating technology (CrN). The specifications of the engine are described in the Table 3. It is a 4-cylinder turbocharged engine with high peak cylinder pressure with use of low viscosity oil.

The piston rings coated with CrAlN multilayer were placed in the cylinders #1, #3 and #4 while the piston ring of cylinder #2 was kept with the CrN coating for reference purposes. A schematic view of the engine assembly is shown in the Figure 11. The engine ran in a durability protocol for

200 hours where 65% is ran in a full power regime (5750 RPM) and 35% is ran in full torque regime (3500 RPM) both with wide open throttle condition.

Table 3 - Engine details.

Engine type	4-cylinder in-line
Displacement	1332 cm³
Bore	70 mm
Stroke	86.5 mm
Ignition order	1-3-4-2
Compression ratio	10,5:1
Nominal power	185 cv @ 5750 rpm
Nominal torque	270 Nm @ 1750 rpm
Peak Cylinder Pressure	12 MPa
Oil	SAE 0W30
Turbocharger	Yes

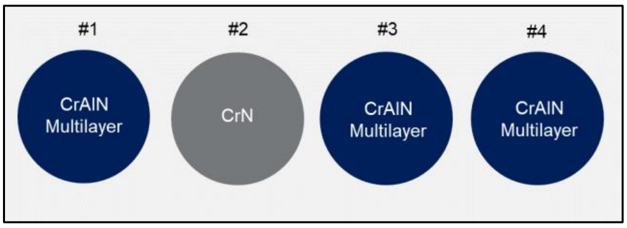

Figure 11 - Engine assembly scheme by coating technology.

PERFORMANCE CHECK – Figure 12 presents the blow-by flow rate map, illustrating the correlation between engine speed, torque and blow-by volume (L/min). The color-coded contour plot highlights regions of equal blow-by, with blue indicating minimal flow (≤5 L/min) and red representing the highest measured values (≥60 L/min). Three distinct operating conditions are overlaid: Wide Open Throttle (WOT), Partial Load, and No Load. The data reveal that blow-by increases significantly at high torque and speed, reaching a peak of 59 L/min—below the reference limit of 65 L/min—while remaining minimal under low-load conditions. This map indicates the piston ring sealing performance was not impacted by the change in coating as expected. It is also shown in the graph that torque curve is within the engine specification of 270 Nm from 1750 to 3750 RPM.

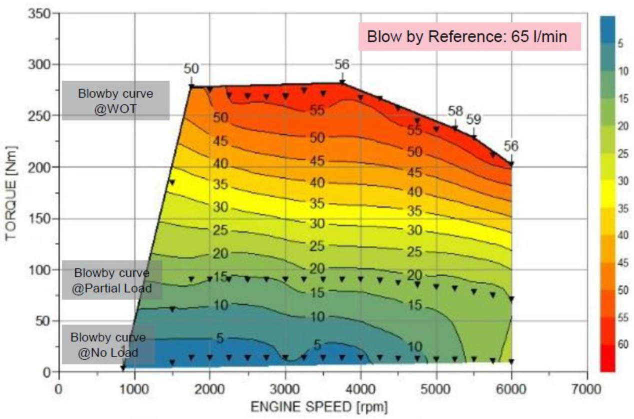

Figure 12 - Blow-by flow rate map

Figure 13 illustrates the lube oil consumption of the engine under three different conditions: Wide Open Throttle (WOT), Partial Load, and after 200 hours of durability testing. The consumption is expressed in grams per hour (g/h) and includes error bars representing measurement uncertainty. At WOT, the engine exhibits the highest oil consumption, approximately 23 g/h, whereas Partial Load operation results in significantly lower consumption, around 7 g/h. After 200 hours of durability testing, the consumption remains controlled at approximately 11 g/h. All measured values are well below the defined limit for each condition as indicated by the dashed red line, demonstrating that the engine maintains efficient oil control performance across different operational conditions and after prolonged use.

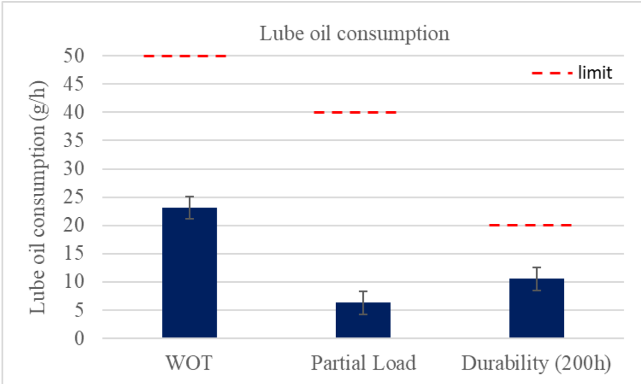

Figure 13 - Lube oil consumption in WOT, partial load and during the durability protocol

VISUAL EVALUATION – The visual evaluation was performed by optical microscopy with image amplification of 100X to 500X and it is the main way to identify the microcracks or spalling occurrences. The Figure 14 presents a representative view of the piston rings contact face from cylinders 1 and 2. The piston ring from cylinder 1 coated with CrAlN multilayer have no traces of microcracks or spalling, only small points that are compatible with the coating porosity. Same observation was made in the rings from cylinders 3 and 4. On the other hand, the piston ring from cylinder 2 presented microcracks along all surface that contacted the cylinder liner and similar to the occurrences reported in the introduction. The absence of microcracks in the CrAlN multilayer coating can be explained by the increase in the resistance to cohesive delamination due to the presence of multiple interfaces produced by the modulation of the aluminum content [3]. The effect of stress barriers to movement of dislocations/microcracks was already reported in NbN/CrN coatings with similar periodicity of 4 nm [29].

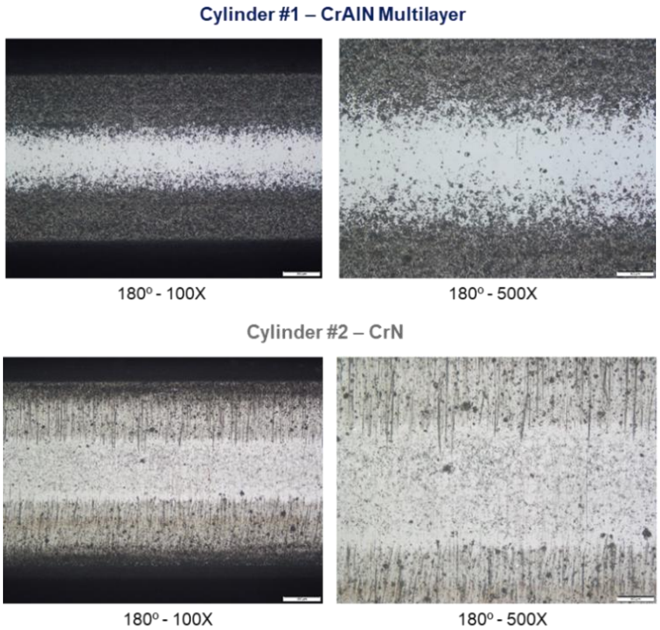

Figure 14 – Visual analysis of piston rings from cylinders #1 (CrAlN) and #2 (CrN) - contact face (100x and 500x) after 200h engine test.

The Figure 15 shows the cylinder liners #1 and #2 after the 200h engine test. The thrust and anti-thrust side are shown. Despite the substantial hardness increase seen for the CrAlN coating, no impact was seen in the cylinder marking pattern. All cylinder liners demonstrated good condition with no scratches or polished areas. It is important to highlight that all piston rings (CrAlN and CrN) had similar surface roughness of Rz2.

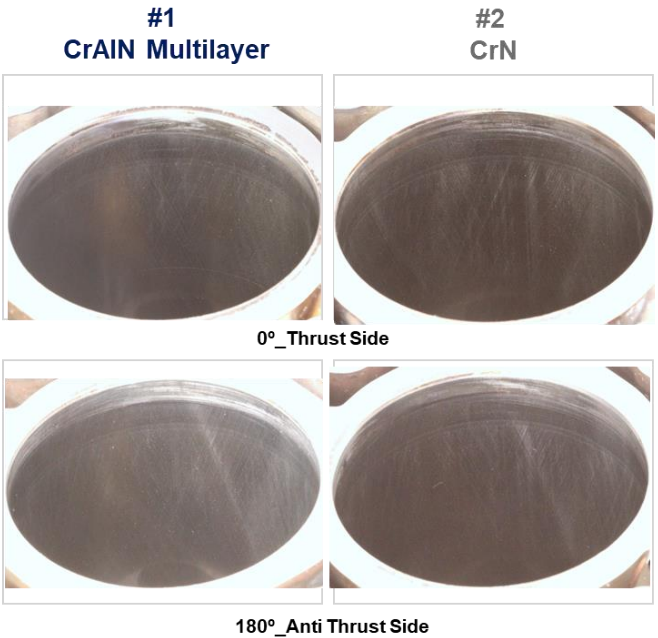

Figure 15 - Visual analysis of cylinders liners #1 (CrAlN multilayer) and #2 (CrN) after 200h engine test.

WEAR EVALUATION – All piston rings were dimensionally inspected before and after the engine test, with the surface profile taken to be able to measure coating wear. Figure 16 shows the top ring wear measurements after the 200h engine test. The wear is presented in micrometers (µm) and evaluated at five circumferential positions: 0°, 90º, 180°, 270º and 360°. Samples #1, #3, and #4 feature CrAlN multilayer coating, while sample #2 is coated with CrN. The wear is higher at the ring tips (0º and 360º) as already expected. Among the CrAlN multilayer samples, wear values generally range between 1.3 and 2.7 µm, with an average of 1.9 µm across all positions. The CrN-coated ring (#2) demonstrates values ranging from 1.4 to 2.9 µm, with an average of 2.0 µm at all measured positions. These results indicate that CrAlN multilayer coating has similar wear performance as the CrN coating.

The results from the engine test differs from the ones found at bench test, where a significant wear reduction was seen. The main hypothesis for that difference is that the conditions at the engine are not that demanding when compared with the wear at bench test, where the load was high with doped oil to accelerate the wear. Therefore, despite the similar wear in comparison with CrN, the CrAlN multilayer has potential to have reduced wear in more demanding conditions. An engine test in a heavy-duty diesel engine is recommended to check wear performance.

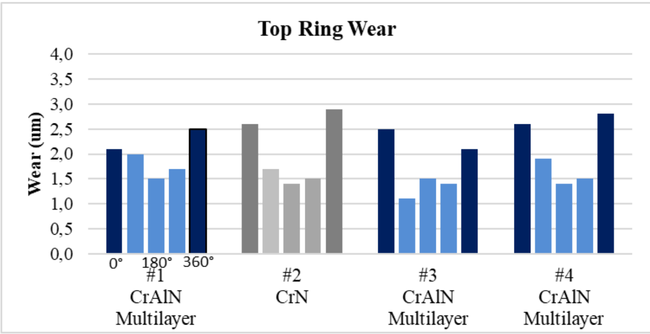

Figure 16 - Top ring wear after 200h engine test.

CONCLUSION

The engines under development to achieve the newest and more restricted emissions and efficiency regulations bring tribological challenges for the current top ring coatings. The CrAlN multilayer coating, produced via cathodic arc deposition, demonstrated superior mechanical properties, including increased hardness and improved wear resistance under controlled bench testing. Its nanolayered design—achieved through modulation of aluminum content—acts as an effective barrier against crack propagation and cohesive failure. An improvement in the scuffing resistance was also seen in bench test.

Engine test confirmed that the CrAlN-coated rings remained free of microcracks and spalling, even under high-load operating conditions using ethanol. Although wear performance was comparable to CrN in this specific application, the results suggest greater potential in more severe environments, such as heavy-duty or high-load diesel engines. In summary, the CrAlN multilayer coating presents a robust and scalable solution for next-generation high-performance flex-fuel engines.

REFERENCES

[1] Ferrarese, A., Marques, G., Tomanik, E., Bruno, R., & Vatavuk, J. (2010). Piston Ring Tribological Challenges on the Next Generation of Flex-fuel Engines. *SAE International Journal of Engines*, *3*(2), 85–91. http://www.jstor.org/stable/26275548

[2] Khuong, L. S., Zulkifli, N. W. M., Masjuki, H. H., Mohamad, E. N., Arslan, A., Mosarof, M. H., & Azham, A. (2016). A review on the effect of bioethanol dilution on the properties and performance of automotive lubricants in gasoline engines. *RSC advances*, *6*(71), 66847-66869. https://doi.org/10.1039/C6RA10003A

[3] Araujo, J. A., Araujo, G. M., Souza, R. M., & Tschiptschin, A. P. (2015). Effect of periodicity on hardness and scratch resistance of CrN/NbN nanoscale multilayer coating deposited by cathodic arc technique. *Wear*, *330*, 469-477. https://doi.org/10.1016/j.wear.2015.01.051

[4] Zhou, Z., Rainforth, W. M., Falke, U., Falke, M., Bleloch, A., & Hovsepian, P. E. (2007). On the structure and composition of nanoscale TiAlN/VN multilayers. *Philosophical Magazine*, *87*(6), 967-978. https://doi.org/10.1080/14786430601019433

[5] Purandare, Y. P., Ehiasarian, A. P., & Hovsepian, P. E. (2008). Deposition of nanoscale multilayer CrN/NbN physical vapor deposition coatings by high power impulse magnetron sputtering. *Journal of Vacuum Science & Technology A*, *26*(2), 288-296. https://doi.org/10.1116/1.2839855

[6] Ljungcrantz, H., Engström, C., Hultman, L., Olsson, M., Chu, X., Wong, M. S., & Sproul, W. D. (1998). Nanoindentation hardness, abrasive wear, and microstructure of TiN/NbN polycrystalline nanostructured multilayer films grown by reactive magnetron sputtering. *Journal of Vacuum Science & Technology A: Vacuum, Surfaces, and Films*, *16*(5), 3104-3113. https://doi.org/10.1116/1.581466

[7] Selinder, T. I., Sjöstrand, M. E., Nordin, M., Larsson, M., Östlund, Å., & Hogmark, S. (1998). Performance of PVD TiN/TaN and TiN/NbN superlattice coated cemented carbide tools in stainless steel machining. *Surface and coatings technology*, *105*(1-2), 51-55. https://doi.org/10.1016/S0257-8972(98)00446-0

[8] Zhitomirsky, V. N., Grimberg, I., Rapoport, L., Travitzky, N. A., Boxman, R. L., Goldsmith, S., & Weiss, B. Z. (1999). Vacuum arc deposition of TiN, NbN and TiN/NbN multi-layer coatings. *Surface and Coatings Technology*, *120*, 219-225. https://doi.org/10.1016/S0257-8972(99)00382-5

[9] Mani, S. P., Agilan, P., Kalaiarasan, M., Ravichandran, K., Rajendran, N., & Meng, Y. (2022). Effect of multilayer CrN/CrAlN coating on the corrosion and contact resistance behavior of 316L SS bipolar plate for high temperature proton exchange membrane fuel cell. *Journal of Materials Science & Technology*, *97*, 134-146. https://doi.org/10.1016/j.jmst.2021.04.043

[10] Setoyama, M., Nakayama, A., Tanaka, M., Kitagawa, N., & Nomura, T. (1996). Formation of cubic-A1N in TiN/A1N superlattice. *Surface and Coatings Technology*, *86*, 225-230. https://doi.org/10.1016/S0257-8972(96)03033-2

[11] Münz, W. D., Donohue, L. A., & Hovsepian, P. E. (2000). Properties of various large-scale fabricated TiAlN- and CrN-based superlattice coatings grown by combined cathodic arc–unbalanced magnetron sputter deposition. *Surface and Coatings Technology*, *125*(1-3), 269-277. https://doi.org/10.1016/S0257-8972(99)00572-1

[12] Wadsworth, I., Smith, I. J., Donohue, L. A., & Münz, W. D. (1997). Thermal stability and oxidation resistance of TiAlN/CrN multilayer coatings. *Surface and Coatings Technology*, *94*, 315-321. https://doi.org/10.1016/S0257-8972(97)00353-8

[13] Luo, Q., Rainforth, W. M., & Münz, W. D. (1999). TEM observations of wear mechanisms of TiAlCrN and TiAlN/CrN coatings grown by combined steered-arc/unbalanced magnetron deposition. *Wear*, *225*, 74-82. https://doi.org/10.1016/S0043-1648(99)00049-6

[14] Mendibide, C., Steyer, P., Fontaine, J., & Goudeau, P. (2006). Improvement of the tribological behaviour of PVD nanostratified TiN/CrN coatings—An explanation. *Surface and Coatings Technology*, *201*(7), 4119-4124. https://doi.org/10.1016/j.surfcoat.2006.08.013

[15] Kadlec, S., Musil, J., Valvoda, V., Münz, W. D., Petersein, H., & Schroeder, J. (1990). TiN films grown by reactive magnetron sputtering with enhanced ionization at low discharge pressures. *Vacuum*, *41*(7-9), 2233-2238. https://doi.org/10.1016/0042-207X(90)94233-G

[16] Hovsepian, P. E., Lewis, D. B., Luo, Q., & Farinotti, A. (2005). Corrosion resistance of CrN/NbN superlattice coatings grown by various physical vapour deposition techniques. *Thin Solid Films*, *488*(1-2), 1-8. https://doi.org/10.1016/j.tsf.2005.03.016

[17] Lewis, D. B., Reitz, D., Wüstefeld, C., Ohser-Wiedemann, R., Oettel, H., Ehiasarian, A. P., & Hovsepian, P. E. (2006). Chromium nitride/niobium nitride nano-scale multilayer coatings deposited at low temperature by the combined cathodic arc/unbalanced magnetron technique. *Thin Solid Films*, *503*(1-2), 133-142. https://doi.org/10.1016/j.tsf.2005.08.369

[18] Savisalo, T., Lewis, D. B., Luo, Q., Bolton, M., & Hovsepian, P. (2008). Structure of duplex CrN/NbN coatings and their performance against corrosion and wear. *Surface and Coatings technology*, *202*(9), 1661-1667. https://doi.org/10.1016/j.surfcoat.2007.07.024

[19] Bemporad, E., Pecchio, C., De Rossi, S., & Carassiti, F. (2004). Characterisation and wear properties of industrially produced nanoscaled CrN/NbN multilayer coating. *Surface and Coatings Technology*, *188*, 319-330. https://doi.org/10.1016/j.surfcoat.2004.08.069

[20] Ronkainen, H., Vihersalo, J., Varjus, S., Zilliacus, R., Ehrnstén, U., & Nenonen, P. (1997). Improvement of aC: H film adhesion by intermediate layers and sputter cleaning procedures on stainless steel, alumina and cemented carbide. *Surface and Coatings Technology*, *90*(3), 190-196. https://doi.org/10.1016/S0257-8972(96)03131-3

[21] Chen, C. C., & Hong, F. C. N. (2005). Interfacial studies for improving the adhesion of diamond-like carbon films on steel. *Applied Surface Science*, *243*(1-4), 296-303. https://doi.org/10.1016/j.apsusc.2004.09.085

[22] Anders, A. (2002). Cathodic arc plasma deposition. *Vacuum Technology & Coating*, *3*, n. 7, 27–35 https://escholarship.org/uc/item/33n1m86d

[23] Meng-Burany, X., & Alpas, A. T. (2007). FIB and TEM studies of damage mechanisms in DLC coatings sliding against aluminum. Thin Solid Films, 516(2-4), 325-335. https://doi.org/10.1016/j.tsf.2007.06.038

[24] Oliver, W. C., & Pharr, G. M. (1992). An improved technique for determining hardness and elastic modulus using load and displacement sensing indentation experiments. *Journal of materials research*, *7*(6), 1564-1583. https://doi.org/10.1557/JMR.1992.1564

[25] Ferreira, R., Martins, J., Carvalho, Ó., Sobral, L., Carvalho, S., & Silva, F. (2019). Tribological solutions for engine piston ring surfaces: an overview on the materials and manufacturing. *Materials and Manufacturing Processes*, *35*(5), 498–520. https://doi.org/10.1080/10426914.2019.1692352

[26] Ding, X. Z., & Zeng, X. T. (2005). Structural, mechanical and tribological properties of CrAlN coatings deposited by reactive unbalanced magnetron sputtering. *Surface and Coatings Technology*, *200*(5-6), 1372-1376. https://doi.org/10.1016/j.surfcoat.2005.08.072

[27] Yashar, P. C., & Sproul, W. D. (1999). Nanometer scale multilayered hard coatings. *Vacuum*, *55*(3-4), 179-190. https://doi.org/10.1016/S0042-207X(99)00148-7

[28] Araujo, J. A., Souza, R. M., Lima, N. B. D., & Tschiptschin, A. P. (2016). Thick CrN/NbN multilayer coating deposited by cathodic arc technique. *Materials Research*, *20*, 200-209. https://doi.org/10.1590/1980-5373-MR-2016-0293

[29] Araujo, J. A., Giorjão, R. A. R., Bettini, J., Souza, R. M., & Tschiptschin, A. P. (2016). Modeling intrinsic residual stresses built-up during growth of nanostructured multilayer NbN/CrN coatings. *Surface and Coatings Technology*, *308*, 264-272. https://doi.org/10.1016/j.surfcoat.2016.07.108

[30] de Castilho, B. C. N. M., Rodrigues, A. M., Avila, P. R. T., Apolinario, R. C., Nossa, T. D. S., Walczak, M., ... & Pinto, H. C. (2022). Hybrid magnetron sputtering of ceramic superlattices for application in a next generation of combustion engines. *Scientific Reports*, *12*(1), 2342. https://doi.org/10.1038/s41598-022-06131-9

[31] Mazuco, F. S., Rezende, L. F. V. R., Araujo, J. A., Pereira, J. I., & Souza, R. M. (2023). Parameters study of carbon bombardment step for enhanced adhesion of thick DLC coating deposited by cathodic arc evaporation. *Surface and Coatings Technology*, *457*, 129310. https://doi.org/10.1016/j.surfcoat.2023.129310

[32] Obert, P., Müller, T., Füßer, H. J., & Bartel, D. (2016). The influence of oil supply and cylinder liner temperature on friction, wear and scuffing behavior of piston ring cylinder liner contacts–A new model test. *Tribology International*, *94*, 306-314. https://doi.org/10.1016/j.triboint.2015.08.026